remote sensing

MDPI

Communication

An HAP and UAVs Collaboration Framework for Uplink Secure Rate Maximization in NOMA-Enabled IoT Networks

Dawei Wang [1,2,3], Menghan Wu [1,2], Yixin He [1,2], Linna Pang [4,*], Qian Xu [2] and Ruonan Zhang [2]

[1] Research & Development Institute, Northwestern Polytechnical University in Shenzhen, Shenzhen 518057, China
[2] School of Electronics and Information, Northwestern Polytechnical University, Xi'an 710072, China
[3] Dongguan Sanhang Innovation Institute, Dongguan 523808, China
[4] Beijing Research Institute of Telemetry, Beijing 100094, China
* Correspondence: lnpang@ieee.org

Abstract: In this paper, we propose a high-altitude platform (HAP) and unmanned aerial vehicles (UAVs) collaboration framework in non-orthogonal multiple access (NOMA)-enabled Internet of Things (IoT) networks with the presence of an eavesdropping UAV. For the considered framework, we investigate the uplink secure transmission by optimizing channel allocation from UAVs to HAP, users' power, and UAVs' three-dimensional (3D) position. To solve this non-convex problem, we adopt the K-means cluster pair algorithm to divide paired users into different groups and each cluster can be served by a corresponding UAV. Then, the formulated optimization problem is decoupled into three subproblems and tackled iteratively based on the block coordinate descent (BCD) algorithm. Finally, simulation results verify that the proposed network architecture can achieve a higher secure rate, faster convergence evolution, and lower complexity in comparison with the current works.

Keywords: high-altitude platform (HAP); non-orthogonal multiple access (NOMA); Internet of Things (IoT); secure rate; unmanned aerial vehicles (UAVs)

check for updates

Citation: Wang, D.; Wu, M.; He, Y.; Pang, L.; Xu, Q.; Zhang, R. An HAP and UAVs Collaboration Framework for Uplink Secure Rate Maximization in NOMA-Enabled IoT Networks. *Remote Sens.* **2022**, *14*, 4501. https://doi.org/10.3390/rs14184501

Academic Editors: Prem Prakash Jayaraman, Gwanggil Jeon, Federico Montori, Charith Perera and Felip Marti

Received: 10 July 2022
Accepted: 2 September 2022
Published: 9 September 2022

Publisher's Note: MDPI stays neutral with regard to jurisdictional claims in published maps and institutional affiliations.

Copyright: © 2022 by the authors. Licensee MDPI, Basel, Switzerland. This article is an open access article distributed under the terms and conditions of the Creative Commons Attribution (CC BY) license (https://creativecommons.org/licenses/by/4.0/).

1. Introduction

Internet of Things (IoT) networks provide fast and reliable data services by deploying a large number of cheap devices [1,2]. However, massive accesses to wireless devices burden the available wireless spectrum resource. In recent years, unmanned aerial vehicles (UAVs) have been extensively applied to IoT networks for their high mobility, low cost, and on-demand deployment [3]. UAVs can be served as aerial base stations to provide aid in terrestrial network communications [4], and as mobile relays to provide reliable wireless connectivity to remote areas [5]. However, when the ground infrastructure is faulty, a UAV cannot provide long and reliable services due to its limited power and coverage. Therefore, a collaboration framework between high-altitude platforms (HAPs) and UAVs can be designed to form a double-layer three-dimensional (3D) dense coverage network to guarantee the quality of service (QoS) requirements of terrestrial users. Different from traditional base stations, HAPs hovering at high altitude can provide enormous network coverage for terrestrial users [6]. Besides, HAPs have lower construction and maintenance costs compared to the traditional low earth orbit (LEO) satellite [7]. Therefore, an efficient uplink transmission can be achieved in future wireless communications by combining the high coverage of HAPs and high flexibility of UAVs.

The forthcoming sixth generation (6G) communication puts forward higher requirements on the spectral efficiency and throughput of the system due to the exponential growth of network nodes. Mass connectivity and high spectrum utilization of the non-orthogonal multiple access (NOMA) technique can effectively solve the above problems [8]. Multiple users share the same spectrum to transmit data through NOMA, and the successive interference cancellation (SIC) technology is used to decode the transmitted data at

the receiver and ensure the reliability of information transmission [9]. Although the use of a SIC receiver may increase the complexity of the receiver design, it can improve the frequency spectrum efficiency [10].

1.1. Related Works

The authors in [11] considered an emergency communication scenario assisted by a UAV relay based on the NOMA technique. A hybrid uplink problem was investigated in [12] to integrate NOMA into orthogonal multiple access (OMA), in which the authors allocated energy resources efficiently to satisfy the QoS of users. The authors in [13] analyzed the performance of the NOMA-relevant strategy on an uplink network with statistical delay constraints and compared it with NOMA and OMA in terms of energy efficiency. Moreover, the maximum coverage ratio of the double-layer airborne access VANETs network has been researched in [14]. A survey of an airborne communication network including HAP-based, LAP-based, and hybrid UAV-HAP networks was conducted in [15]. The authors in [16] integrated HAP as a reliable relay into the FSO link to achieve higher reliability of the space–air–ground integrated network (SAGIN). A heterogeneous statistical QoS provisioning network was proposed to provide various real-time services in HAP and UAVs [17]. The authors in [18] designed a hierarchical federated learning algorithm to solve the content caching issues between an HAP and multiple UAVs.

Due to the broadcast and line-of-sight nature of the wireless propagation environment, confidential information is vulnerable to eavesdroppers during transmissions. Under this condition, the security of NOMA-enabled IoT networks cannot be guaranteed. However, Refs. [11–13] did not consider the coverage capability of UAVs and the HAP collaboration framework. Moreover, the NOMA technology is not introduced to improve the spectrum efficiency of the network in [15–18]. Furthermore, all of the above authors ignore the information security issue of uplink transmissions caused by the instability and vulnerability of wireless channels.

1.2. Contributions

Recently, the physical layer security (PLS) has emerged as a promising effective technique to realize secrecy in IoT wireless communication [19,20]. Motivated by the above, in this paper, we propose an HAP and UAVs collaboration framework in NOMA-enabled networks with the presence of an eavesdropping (EVE) UAV. The main contributions are summarized as follows.

- We employ the PLS technique to investigate the uplink secure rate maximization problem by joint considering channel allocation from UAVs to the HAP, users' power control, and UAVs' 3D position.
- In order to improve the spectrum utilization of NOMA-enabled networks, we propose a NOMA pairing scheme based on the K-means clustering algorithm. Then, by exploiting the block coordinate descent (BCD) algorithm, the formulated optimization problem is decoupled into three subproblems. Afterward, an iterative algorithm is designed, where three optimization variables are tackled in turn.
- Finally, simulation results show that our designed algorithm improves the uplink secure rate, reduces complexity, and speeds up the rate of convergence.

1.3. Organization

The rest of this paper is organized as follows. In Section 2, the focused system model and problem formulation are introduced. Section 2 presents the secure rate maximization scheme by jointly optimizing the position deployment of UAVs, the power control of users, and the subcarrier schedule. The simulation results are illustrated in Section 2 and the conclusion is given in Section 2.

2. System Model and Problem Formulation

2.1. System Model

In this paper, we consider a double-layer cooperated network involving one HAP and mutiple UAVs. As shown in Figure 1, the users are divided into M clusters, each of which is served by a UAV in an independent channel. The ID set of UAVs and channels are denoted by $\mathbf{M} = \{1, 2, \ldots, m, \ldots, M\}$ and $\mathbf{K} = \{1, 2, \ldots, k, \ldots, K\}$, respectively. The total channel bandwidth is B, and the bandwidth of subchannel k is $B_t = B/K$. In order to improve the spectrum utilization of the system, we form the adjacent user and the distant user with respect to the UAV as a NOMA pair who transmit data in the same subcarrier B_p, where $B_p = B_t/N_p$ means there are N_p NOMA pairs in a cluster and each pair links to only one subcarrier. The data is first transmitted from users to the UAV in the first phase, and then the UAV forwards it to the HAP using decode-and-forward (DF) protocol in the second phase. Because of the broadcast and vulnerability of wireless channel, we consider a case that there is a passive EVE attempting to make wiretap and spoof threats during the two phases. The 3D position of the HAP, UAV, EVE, the adjacent user, and the distant user are denoted by $[x_h, y_h, H]$, $[x_u, y_u, h_u]$, $[x_e, y_e, h_e]$, $[x_a, y_a, 0]$, and $[x_d, y_d, 0]$, respectively.

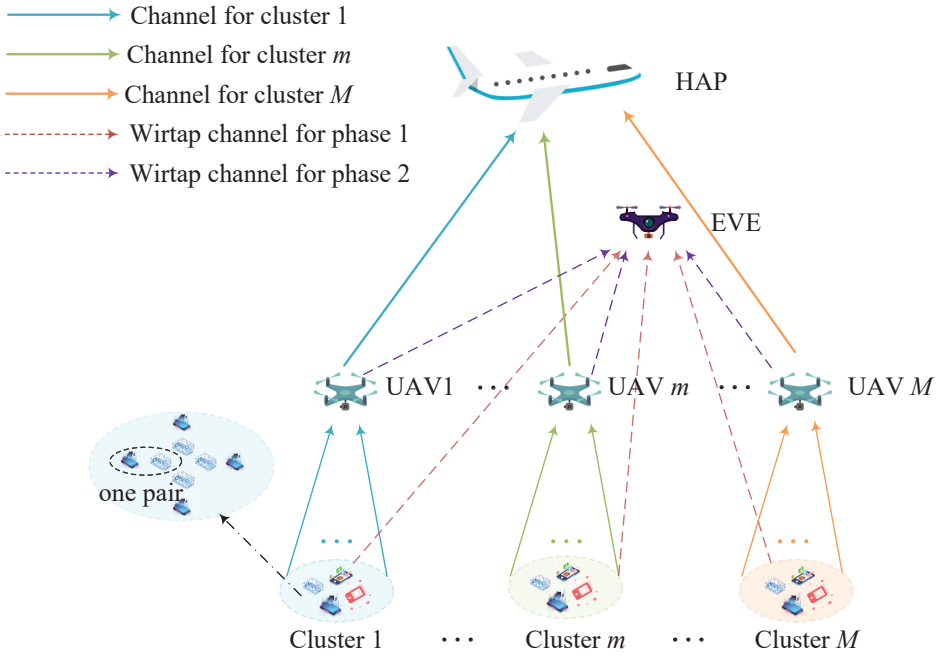

Figure 1. An HAP and UAVs collaboration framework in NOMA-enabled networks.

The low-altitude air-to-ground (ATG) channel in the first phase is more complex than the high-altitude channel and traditional terrestrial mobile access channel due to its variability. Therefore, this paper considers a practical urban macrocell (UMa) model measured by our team to express the path loss (PL) in users–UAV links [21], i.e.,

$$\begin{aligned} \mathrm{PL}_{\mathrm{DU}} = {} & 28.0 + 22\lg(d_{\mathrm{DU}}[\mathrm{m}]) + 20\lg(f_c[\mathrm{GHz}]) \\ & + 1.0005 \times 10^{-4} h_u^2 - 0.0286 h_u + 10.5169, \end{aligned} \tag{1}$$

where d_{DU} is the Euclidean distance from the user to the UAV, and f_c is the center frequency of the signal.

In addition, due to the strong line-of-sight (LOS) propagation in the UAV-HAP phase, the pass loss in this stage can be expressed based on the 3GPP UMa model [22], i.e.,

$$\mathrm{PL}_{\mathrm{UH}} = 32.44 + 20\lg(d_{\mathrm{UH}}[\mathrm{m}]) + 20\lg(\mathrm{f_c}[\mathrm{GHz}]), \tag{2}$$

where d_{UH} is the Euclidean distance from the UAV to HAP.

The achievable rate from the adjacent user and the distant user in NOMA pair to the UAV or EVE can be expressed as

$$r_a^{D\to X} = B_p \log_2\left(1 + \frac{P_a G_a^{D\to X}}{P_d G_d^{D\to X} + \sigma_1^2}\right), \tag{3}$$

and

$$r_d^{D\to X} = B_p \log_2\left(1 + \frac{P_d G_d^{D\to X}}{\sigma_1^2}\right), \tag{4}$$

where P_a and P_d are the transmit power of adjacent user and distant user, respectively. $X = \{\mathrm{U}, \mathrm{E}\}$ represents UAV or EVE, respectively, $\sigma_1^2 = B_p N_0$ is the variance of the additional white Gaussian noise in the first phase. Similarly, the achievable rate from UAV to EVE or HAP can be respectively expressed as

$$r^{U\to X} = B_t \log_2\left(1 + \frac{P_u G^{U\to X}}{\sigma_2^2}\right), \tag{5}$$

where P_u and $G^{U\to X}$ $(X = \{\mathrm{H}, \mathrm{E}\})$ are the UAVs' transmission power and the channel gain from UAV to HAP or EVE, respectively, and $\sigma_2^2 = B_t N_0$ is the variance of the additional white Gaussian noise in the second phase. Therefore, as discussed in [23], the secure rate of adjacent user and distant user can be expressed as

$$r_x^{\mathrm{sec}} = \min\{\left[r_x^{D\to U} - r_x^{D\to E}\right]^+, \left[r^{U\to H} - r^{U\to E}\right]^+\}, \tag{6}$$

where $[\Lambda]^+ \triangleq \max(\Lambda, 0)$ and $x = \{\mathrm{a}, \mathrm{d}\}$ represents the adjacent user and distant user, respectively. Hence, the sum secure rate in a NOMA pair R_p^{sec} is $R_p^{\mathrm{sec}} = r_a^{\mathrm{sec}} + r_d^{\mathrm{sec}}$. Table 1 lists the notations used in this paper.

Table 1. Notations.

Symbol	Definition
$\mathbf{M} = \{1, 2, \ldots, m, \ldots, M\}$	set of UAVs or clusters
$\mathbf{K} = \{1, 2, \ldots, k, \ldots, K\}$	set of channels
$\mathbf{N_p} = \{1, 2, \ldots, p, \ldots, N_p\}$	set of NOMA pairs
B	total channel bandwidth
B_t	subchannel bandwidth of a cluster
B_p	subchannel bandwidth of a NOMA pair
P_a/P_d	transmit power of adjacent/distant user
$P_{\max}$	maximum transmit power of users
P_u	transmit power of UAVs
h_u	height of UAVs
$h_{\min}/h_{\max}$	minimum/maximum height of UAVs
$G_u^{U\to X}$	channel power gain from UAVs to HAP or EVE
$G_d^{D\to X}$	channel power gain from distant user to UAV or EVE
$\mathrm{PL_{DU}}/\mathrm{PL_{UH}}$	path loss in user–UAV/UAV–HAP links
D_{DU}	Euclidean distance from the user to the UAV
D_{UH}	Euclidean distance from the UAV to the HAP
i	iteration of the K-means cluster pair algorithm
$\mathbf{Q}$	2D coordinates of UAVs

2.2. Problem Formulation

It is expected to maximize the total secure rate by optimzing channel allocation from UAVs to HAP, users' power, and UAVs' 3D position. The optimization problem is formulated as

$$\mathrm{P1}: \max_{\mathbf{A},\mathbf{P},\mathbf{H},\mathbf{Q}} \sum_{m=1}^{M}\sum_{k=1}^{K}\sum_{p=1}^{N_p} a_{m,k} R_p^{\mathrm{sec}}, \tag{7}$$

$$\text{s.t.} \sum_{m=1}^{M}\sum_{k=1}^{K} a_{m,k} \leqslant 1, \tag{8}$$

$$a_{m,k} \in \{0,1\}, \forall m, \forall k, \tag{9}$$

$$0 \leqslant P_a \leqslant P_{\max}, \forall n \in \mathrm{N}, \tag{10}$$

$$0 \leqslant P_d \leqslant P_{\max}, \forall n \in \mathrm{N}, \tag{11}$$

$$h_{\min} \leqslant h_u \leqslant h_{\max}, \forall m \in \mathrm{M}, \tag{12}$$

where $\mathbf{A} = \left\{a_{m,k}\right\}_{\forall m,\forall k}$, $\mathbf{P} = \left\{P_{a/d}\right\}_{a,d\in N_p}$, $\mathbf{H} = \left\{h_u\right\}_{u\in M}$, and $\mathbf{Q} = \left\{x_u, y_u\right\}_{u\in M}$. In P1, $a_{m,k}$ is a binary variable. If UAV_m is served by HAP in channel k, $a_{m,k} = 1$, otherwise $a_{m,k} = 0$. In addition, $P_{\max}$ is the maximum transmit power of the users, and $h_{\min}$ and $h_{\max}$ are the altitude constraint of UAVs.

3. Secure Rate Maximization Scheme

In this section, we first use the K-means cluster pair algorithm to obtain the UAV's 2D coordinates $\mathbf{Q}$ and the user's pairing mode. Then, given the UAV's 2D coordinates, we optimize the channel allocation from the UAVs to the HAP, the users' power, and the UAVs' height, respectively. Afterward, the BCD iterative algorithm is proposed to obtain the optimal secure rate.

3.1. K-Means Cluster Pair Algorithm

The detailed process of the K-means pair cluster algorithm is shown in Algorithm 1. This algorithm can maximize the total secure rate by reducing the horizontal Euclidean distance between the UAV and users. Afterward, the centroid of the clusters is set to be the UAVs' optimal horizontal coordinate $\mathbf{Q}^*$ and the NOMA pair is also determined, where such a setting is optimal regardless of how the channel, power, and height change [24].

Algorithm 1 K-means cluster pair algorithm

1: Set $i = 0$ and choose M points as the initial center, $\mathrm{center}_m^0 \in \left\{\mathrm{center}_1^0, \mathrm{center}_2^0, ..., \mathrm{center}_M^0\right\}$.
2: **repeat**
3: Compute the distance from users to $\mathrm{center}_m^i, m = 1, 2, ..., M$.
4: Sort the users close to center_m^i into $\mathrm{cluster}_m$, where the mean value of those sorted users' coordinates is the new center of $\mathrm{cluster}_m$ denoted by center_m^{i+1}.
5: $i = i + 1$.
6: **until** convergence.
7: The UAV_m's horizontal coordinates is ${\mathrm{center}_m}^{i+1}$
8: Categorize half of the users closest to the UAV as adjacent users and others as distant users .
9: **repeat**
10: Calculate the distance between the distant users and the adjacent users.
11: The one with the shorter distance is formed as a NOMA pair and will be removed in the next calculation.
12: **until** Each distant user matches an adjacent user.

3.2. Resource Allocation

First, given the optimal horizontal coordinates of UAVs $\mathbf{Q}^*$, it is expected to maximize the total secure rate by optimizing the remaining three variables, $\mathbf{A}, \mathbf{P}, \mathbf{H}$. Second, the operator $[\bullet]^+$, making the objective functions of P1 nonsmooth at zero value, can be omitted in the optimal case which has been proved in detail in Lemma 1 of [25]. Thus, the original problem can be written as follows:

$$\begin{aligned} \text{P2}: \quad & \max_{\mathbf{A},\mathbf{P},\mathbf{H}} \sum_{m=1}^{M} \sum_{k=1}^{K} \sum_{p=1}^{N_p} a_{m,k} \hat{R}_p^{\text{sec}}, \\ & \text{s.t.} (8), (9), (10), (11), (12), \end{aligned} \tag{13}$$

where $\hat{R}_p^{\text{sec}} = \min\left\{ \left[r_a^{D\to U} - r_a^{D\to E} \right], [r_U - r_E] \right\} + \min\left\{ \left[r_d^{D\to U} - r_d^{D\to E} \right], [r_U - r_E] \right\}$. Since the problem P2 is obviously a non-deterministic polynomial (NP)-hard problem with three coupled variables, whose analytical solution is difficult to find, hence we use the BCD algorithm, a typical deterministic method for dealing with non-convex issues [26–28], to decouple the original problem into three subproblems.

3.2.1. Channel Allocation

Initially, the users' transmission power and UAVs' height are fixed to optimize the channel allocation, the binary factor $a_{m,k}$ is slacked to continuous variables $\hat{a}_{m,k}$ and the optimization problem P2 can be written as

$$\text{P3.1}: \max_{\mathbf{A}} \quad \sum_{m=1}^{M} \sum_{k=1}^{K} \sum_{p=1}^{N_p} \hat{a}_{m,k} \hat{R}_p^{\text{sec}}, \tag{14}$$

$$\text{s.t.} \quad \sum_{m=1}^{M} \sum_{k=1}^{K} \hat{a}_{m,k} \leqslant 1, \hat{a}_{m,k} \in [0,1], \forall m, \forall k. \tag{15}$$

It is obvious that problem P3.1 is a linear programming problem and can be solved by MATLAB toolbox CVX. This relaxation technique can transform the integer program optimization problem into a linear programming problem, where the decimal solution of the relaxed linear program is the upper limit of the original problem and consequently the ultimate integer solution can be obtained by relaxation transform.

3.2.2. Power Optimization

In this stage, the transmission power of users is optimized with the channel allocation and height of UAVs fixed. The secure rate in the first phase of a NOMA pair $\hat{R}_p^{1,\text{sec}}$ can be expressed as

$$\begin{aligned} \hat{R}_p^{1,\text{sec}} =& \left(r_a^{D\to U} - r_a^{D\to E} \right) + \left(r_d^{D\to U} - r_d^{D\to E} \right) \\ =& B_p \log_2 \left(\frac{T(d,U) + \sigma_1^2 + T(a,U)}{T(d,U) + \sigma_1^2} \right) \\ & - B_p \log_2 \left(\frac{T(d,E) + \sigma_1^2 + T(a,E)}{T(d,E) + \sigma_1^2} \right) \\ & + B_p \log_2 \left(\frac{\sigma_1^2 + T(d,U)}{\sigma_1^2} \right) - B_p \log_2 \left(\frac{\sigma_1^2 + T(d,E)}{\sigma_1^2} \right) \\ =& B_p \log_2 \Big(T(d,U) + \sigma_1^2 + T(a,U) \Big) \\ & - B_p \log_2 \Big(T(d,E) + \sigma_1^2 + T(a,E) \Big), \end{aligned} \tag{16}$$

where $T(x,Y) = P_x G_x^{D\to Y}$ is the product of signal power and channel gain.

Due to the non-convex nature of the above equation, the successive convex approximation (SCA) method is applied to obtain a convergent solution. The solution at $(l-1)$-th iteration is regarded as the local solution of the l-th iteration. Then, we use first-order Taylor expansion to obtain its lower bound as

$$\begin{aligned}\hat{R}_p^{1,\mathrm{sec}} \geq \tilde{R}_p^{1,\mathrm{sec}} =& B_p \log_2\Big(T(d,U)+\sigma_1^2+T(a,U)\Big)\\ &-\frac{1}{\ln 2}B_p\frac{T(d,E)-T^l(d,E)}{T^l(d,E)+\sigma_1^2+T^l(a,E)}\\ &-\frac{1}{\ln 2}B_p\frac{T(a,E)-T^l(a,E)}{T^l(d,E)+\sigma_1^2+T^l(a,E)}\\ &-B_p\log_2\Big(T^l(d,E)+\sigma_1^2+T^l(a,E)\Big)\end{aligned} \tag{17}$$

where l represents the l-th iteration. Then, the original problem can be converted into the following convex problem

$$\begin{aligned}\text{P3.2}: \quad &\max_{\mathbf{P}} \sum_{m=1}^{M}\sum_{k=1}^{K}\sum_{p=1}^{N_p} \min\Big\{\tilde{R}_p^{1,\mathrm{sec}}, \hat{R}_p^{2,\mathrm{sec}}\Big\},\\ &\text{s.t. } (10), (11),\end{aligned} \tag{18}$$

where $\hat{R}_p^{2,\mathrm{sec}}$ is the secure rate in second phase of a NOMA pair. Hence, such a problem can be solved using the CVX toolbox in MATLAB.

3.2.3. Height Optimization

With fixed channel and power allocation, the height optimization problem can be converted to

$$\begin{aligned}\text{P3.3}: \max_{\mathbf{H}} \quad &\sum_{m=1}^{M}\sum_{k=1}^{K}\sum_{p=1}^{N_p} \hat{R}_p^{\mathrm{sec}},\\ \text{s.t.} \quad &(12).\end{aligned} \tag{19}$$

The UAVs' height affects the total secure rate in both time slots. The influence can be interpreted as: $r_x^{D\to U}$ increases when UAV is closer to the ground and $r^{U\to H}$ decreases at the second phase. Here the ant colony optimization (ACO) algorithm is applied to address the optimal height of UAVs [29].

The ACO algorithm has three important parameters which are pheromone volatile factor ρ, transfer probability constant P_0, and local search step size μ. In order to obtain the optimum altitude by using ACO, the procedures are as follows. Firstly, the height optimization range of the UAV is divided into t discrete points, denoted by h_j, $j=\{1,2,\ldots,t\}$, which are considered as the initial position of the ants. Then, the secure rate calculated at h_j is regarded as the pheromone left by the ant, denoted by R_j. The state transition probability value is obtained from Equation (20), which is given by

$$P=\frac{R_{\max}-R_j}{R_{\max}}, \tag{20}$$

where $R_{\max}$ is the maximum value in the pheromone matrix $\mathbf{R}$, $\mathbf{R}=[R_1,R_2,\ldots,R_t]$.

When P is less than P_0, a local search is performed, otherwise, a global search is performed. Finally, the optimal height of m-th UAV h_m can be addressed accordingly. Specific process is shown in Algorithm 2, where r_1 and r_2 are random numbers for location searches.

Algorithm 2 Height optimization based on ACO algorithm

Initializing: t, ρ, P_0, μ, $h_{\max}$, $h_{\min}$, $iter_{\max}$.
Generate random heights h_j, calculate secure rate R_j.
$iter = 0$.
repeat
  if $P < P_0$ **then**
    $h_j = h_j + \left(r_1 \times \mu \times \frac{1}{iter}\right), r_1 \in [-1, 1]$.
  else
    $h_j = h_j + (r_2 \times (h_{\max} - h_{\min})), r_2 \in [-0.5, 0.5]$.
  end if
  update pheromone: $R_j = (1 - \rho) \times R_j + R(h_j)$.
  $iter = iter + 1$.
until $iter = iter_{\max}$.
Output the optimal height h_m .

3.3. Iterative Algorithm

The iterative procedure can be found in Figure 2. Firstly, we use the K-means cluster pair algorithm to obtain the UAV's 2D coordinates $\mathbf{Q}^*$. Secondly, given the three initial values (channel, power, and height) $\mathbf{A}^{(0)}, \mathbf{P}^{(0)}$ and $\mathbf{H}^{(0)}$, the BCD algorithm is used to decompose the original problem P2 into three subproblems (channel allocation, power optimization and height optimization), each of them is optimized with the remaining two variables fixed. After that, the result of the first iteration is used as the initial value of the second iteration, and we repeat these successive iterations where the maximum secure rate can be obtained due to its convergence. Finally, the optimal channel allocation $\mathbf{A}^*$, optimal transmit power $\mathbf{P}^*$ and optimal UAVs' height $\mathbf{H}^*$ can be derived.

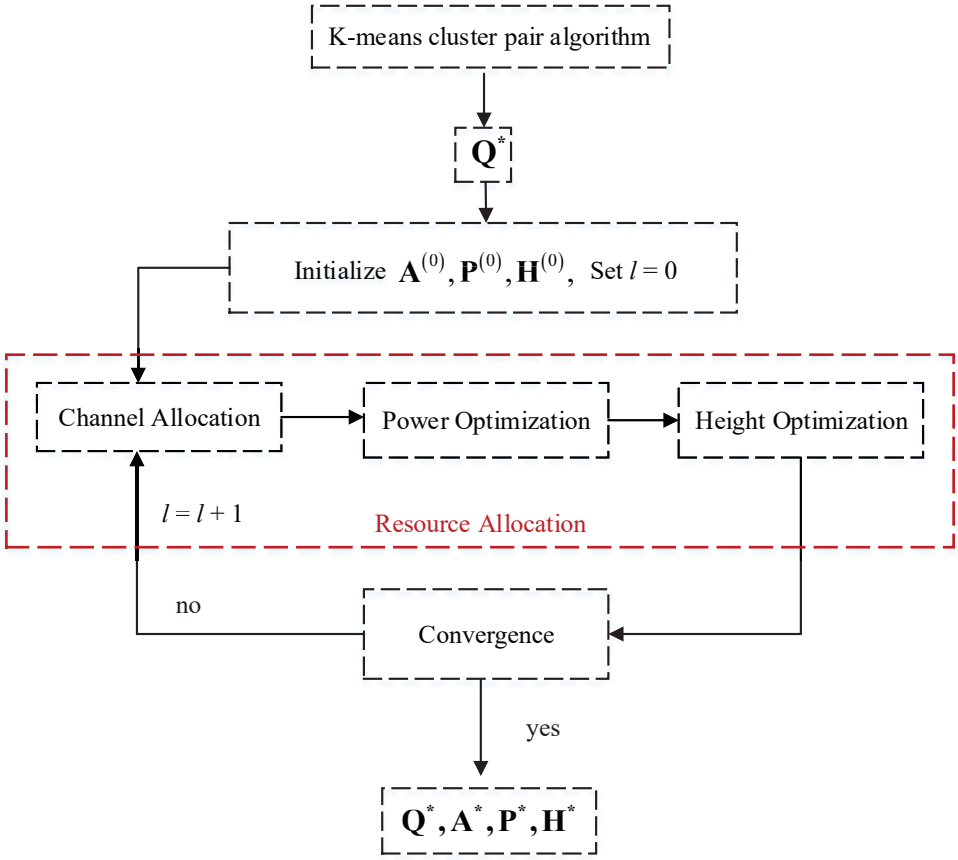

Figure 2. Iterative framework of our proposed algorithm.

In addition, the convergence of the algorithm is proved as follows. First, we can derive an upper bound of the sum secure rate by a simple scenario. We assume that there is only a single user uploading information whose maximum secure rate is $r^{\text{sec}}(\mathbf{H}^*, \mathbf{P}^*)$, where the optimal UAV's altitude $(\mathbf{H}^*)$ and users' power $(\mathbf{P}^*)$ can be obtained by the enumeration method. Then the upper sum sesure rate of an HAP and A UAVs where N users are presented in the coverage area of each UAV is $R^{\text{upper}} = A \times N \times r^{\text{sec}}(\mathbf{H}^*, \mathbf{P}^*)$. Therefore, due to the limited users' power and spectrum bandwidth, our proposed algorithm will gradually converge at the end. Moreover, we consider the convergence is achieved when the difference between the sum secure rate of the $(l+1)$-th iteration and the l-th iteration is less than 10^{-5}.

4. Simulation Experiments

Numerical results are used to verify the effectiveness of the proposed algorithm in this section.

4.1. Initialization

It is assumed that all users are randomly distributed whose amount is 40. More detailed parameters are given in Table 2, and their initial settings are as follows: channel **A** is assigned randomly, power **P** is taken as the maximum value, and the height of the UAV **H** is the middle value between the HAP and users.

Table 2. Simulation Parameters.

Parameter	Value
Number of UAVs, M	4
Number of channels, K	5
Bandwidth of each user, B	180 kHZ
Carrier frequency	2.1 GHz
Coordinates of HAP	$[500, 500, 950]$
Coordinates of EVE	$[400, 800, 500]$
$h_{\min}$ and $h_{\max}$ of UAVs	50/500 m
$P_{\min}$ and $P_{\max}$ of users	0.1/1 W

4.2. Numerical Results

In Figure 3, the optimized positions of UAVs are depicted. To more clearly show the user allocation, the top view of cluster 3 is enlarged. We use the K-means algorithm to divide users into four clusters, with the UAV located at the center of each group to better receive information. Meantime, a distant user and an adjacent one compose a NOMA pair and share the same subcarrier. From Figure 3, we can clearly observe that the UAV tends to be closer to ground users and keeps away from the HAP to achieve a higher total secure rate.

In order to verify the effectiveness of our proposed algorithm, we compared it with the following five algorithms: constant power, constant height, NOMA-relevant [13], NOMA-random, and orthogonal frequency division multiple access (OFDMA). In the constant power scheme, all of the users transmit data at maximum power P_x = 1 Watt. In the constant height scheme, all of the UAVs hover at the same height H_u = 150 m. In the NOMA-relevant scheme, the clusters of users employ NOMA only when it is beneficial for all of them in terms of their individual rates, otherwise the OMA technique is selected. In the NOMA-random scheme, users pair and select spectrum randomly, and in the OFDMA scheme, each user accesses a subchannel independently.

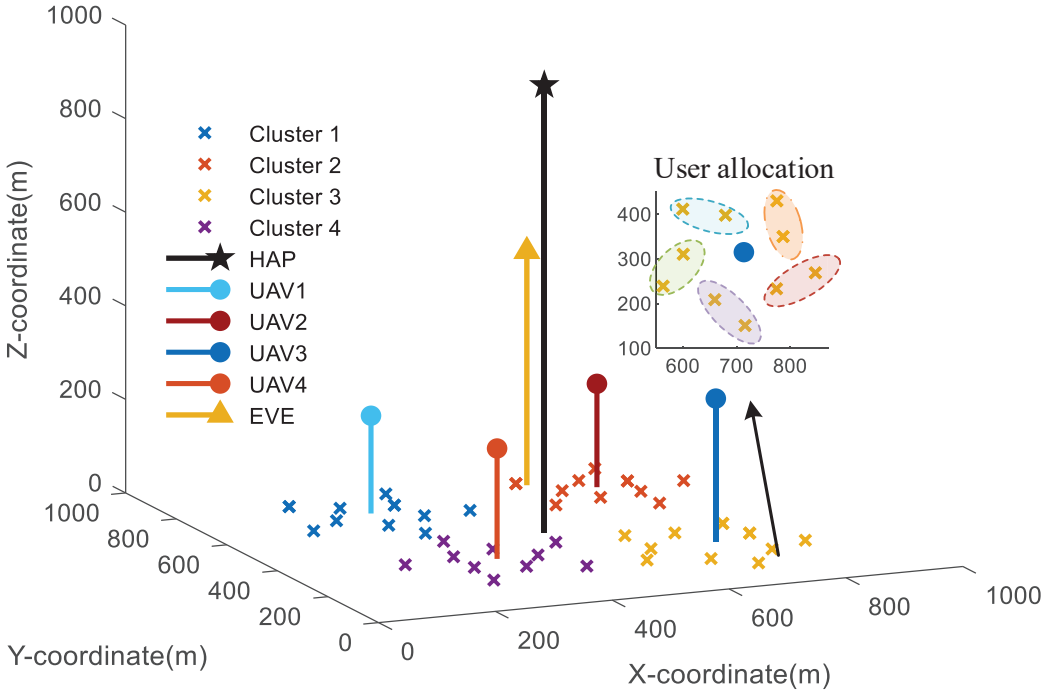

Figure 3. Optimal 3D-locations of UAVs.

Figure 4 shows the relationship between the secure sum rate and the number of iterations. It is observed that our proposed algorithm has faster convergence evolution and achieves better system secure rate improvement. Figure 5 shows the comparison of simulation time with different methods. Although our algorithm takes a long time to implement, it can significantly improve the system performance. Under this condition, the consumption of time cost is reasonable.

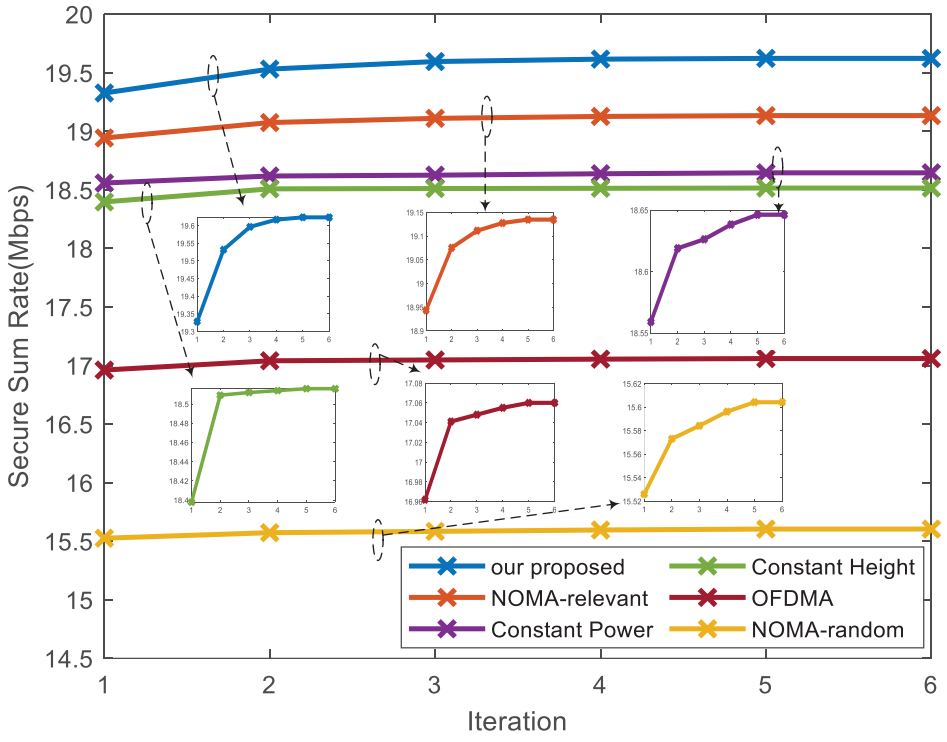

Figure 4. Convergence of different algorithms.

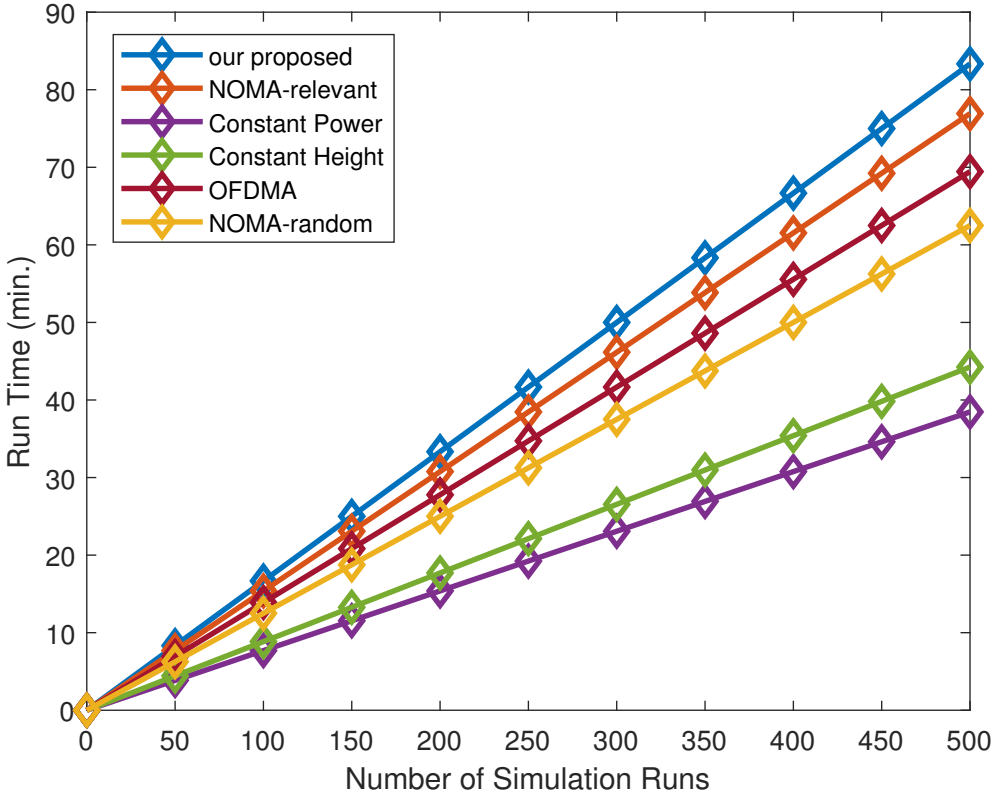

Figure 5. Simulation duration under different algorithms.

4.3. Discussion

Through our above efforts, suboptimal solutions for channel allocation, power optimization, and height optimization are obtained. Our initial optimization problem is an NP-hard problem with a difficult analytical solution to find. Although our algorithm is not optimal, by comparing it with other schemes, our algorithm has the largest sum secure rate, which is effective and guides the way for our future work.

5. Conclusions

In this paper, we proposed an HAP and UAVs collaboration framework in NOMA-enabled IoT networks, based on which the total secure rate maximization problem was investigated. Specifically, the BCD method was used to decouple the joint optimization problem into channel allocation, power optimization, and height optimization subproblems, where the K-means algorithm, SCA and ACO methods were applied to approach the optimal solution. Finally, the demonstration of simulation results indicated the proposed framework can achieve a higher secure rate compared with other existing schemes.

Author Contributions: D.W.: conceptualization, methodology, software, writing—original draft preparation, and visualization. M.W.: conceptualization, resources, writing—review and editing, supervision, project administration, and funding acquisition. Y.H.: conceptualization and writing—review and editing. L.P.: software and formal analysis. Q.X.: software, and formal analysis. R.Z.: conceptualization, resources, supervision, and funding acquisition. All authors have read and agreed to the published version of the manuscript.

Funding: This work was supported in part by the National Natural Science Foundation of China under Grant 62271399 and Grant 61901379, in part by the Key Research and Development Program of Shaanxi Province under Grant 2022KW-07, in part by the National Key Research and Development Program of China under Grant 2020YFB1807003, and in part by the Foundation of the Science, Technology, and Innovation Commission of Shenzhen Municipality under Grant JCYJ20190806160218174.

Data Availability Statement: Not applicable.

Conflicts of Interest: The authors declare no conflict of interest for publishing in this journal.

References

1. Korala, H.; Georgakopoulos, D.; Jayaraman, P.P.; Yavari, A. Managing Time-Sensitive IoT Applications via Dynamic Application Task Distribution and Adaptation. *Remote Sens.* **2021**, *13*, 4148. [CrossRef]
2. Wei, Z.; Masouros, C.; Liu, F.; Chatzinotas, S.; Ottersten, B. Energy- and Cost-Efficient Physical Layer Security in the Era of IoT: The Role of Interference. *IEEE Commun. Mag.* **2020**, *58*, 81–87. [CrossRef]
3. Aggarwal, S.; Kumar, N.; Tanwar, S. Blockchain-envisioned UAV communication using 6G networks: Open issues, use cases, and future directions. *IEEE Internet Things J.* **2021**, *8*, 5416–5441. [CrossRef]
4. Wu, Q.; Zeng, Y.; Zhang, R. Joint trajectory and communication design for multi-UAV enabled wireless networks. *IEEE Trans. Wirel. Commun.* **2018**, *17*, 2109–2121. [CrossRef]
5. Zeng, Y.; Zhang, R.; Lim, T.J. Throughput maximization for UAV-enabled mobile relaying systems. *IEEE Trans. Commun.* **2016**, *64*, 4983–4996. [CrossRef]
6. Wang, D.; He, Y.; Yu, K.; Srivastava, G.; Nie, L.; Zhang, R. Delay-Sensitive Secure NOMA Transmission for Hierarchical HAP–LAP Medical-Care IoT Networks. *IEEE Trans. Ind. Inf.* **2022**, *18*, 5561–5572. [CrossRef]
7. Konishi, M.; Nishimaki, T.; Shibata, Y.; Nabatame, S.; Nagate, A. An experimental study of uplink co-channel spectrum-sharing system between HAPS and terrestrial mobile communication networks. In Proceedings of the 2020 IEEE 92nd Vehicular Technology Conference (VTC2020-Fall), Victoria, BC, Canada, 18 November–16 December 2020; pp. 1–5. [CrossRef]
8. Wang, D.; Zhou, F.; Lin, W.; Ding, Z.; Al-Dhahir, N. Cooperative Hybrid Nonorthogonal Multiple Access-Based Mobile-Edge Computing in Cognitive Radio Networks. *IEEE Trans. Cogn. Commun. Netw.* **2022**, *8*, 1104–1117.
9. Feng, W.; Tang, J.; Zhao, N.; Fu, Y.; Zhang, X. NOMA-based UAV-aided networks for emergency communications. *China Commun.* **2020**, *11*, 54–66. [CrossRef]
10. Wang, J.; Liu, M.; Sun, J.; Gui, G.; Gacanin, H. Multiple unmanned-aerial-vehicles deployment and user pairing for nonorthogonal multiple access schemes. *IEEE Internet Things J.* **2021**, *6*, 1883–1895.
11. Hu, B.; Wang, L.; Chen, S.; Cui, J.; Chen, L. An uplink throughput optimization scheme for UAV-enabled urban emergency communications. *IEEE Internet Things J.* **2022**, *9*, 4291–4302. [CrossRef]
12. Zeng, M.; Yadav, A.; Dobre, O.A.; Poor, H.V. Energy-efficient joint user-RB association and power allocation for uplink hybrid NOMA-OMA. *IEEE Internet Things J.* **2019**, *6*, 5119–5131. [CrossRef]
13. Pischella, M.; Chorti, A.; Fijalkow, I. Performance analysis of uplink NOMA-relevant strategy under statistical delay QoS constraints. *IEEE Wirel. Commun. Lett.* **2020**, *9*, 1323–1326. [CrossRef]
14. He, Y.; Nie, L.; Guo, T.; Kaur, K.; Hassan, M.M.; Yu, K. A NOMA-Enabled Framework for Relay Deployment and Network Optimization in Double-Layer Airborne Access VANETs. *IEEE Trans. Intell. Transp. Syst.* **2022**. [CrossRef]
15. Cao, X.; Yang, P.; Alzenad, M.; Xi, X.; Wu, D.; Yanikomeroglu, H. Airborne communication networks: A survey. *J. Sel. Areas Commun.* **2018**, *36*, 1907–1926. [CrossRef]
16. Ramabadran, S.; Sharma, S.; Vishwakarma, N.; Madhukumar, A.S. HAPS-based relaying for integrated space–air–ground networks with hybrid FSO/RF communication: A performance analysis. *Trans. Aerosp. Electron. Syst.* **2021**, *57*, 1581–1599. [CrossRef]
17. Zhang, X.; Cheng, W.; Zhang, H. Heterogeneous statistical QoS provisioning over airborne mobile wireless networks. *IEEE J. Sel. Areas Commun.* **2018**, *36*, 2139–2152.
18. Masood, A.; Nguyen, T.-V.; Truong, T.P.; Cho, S. Content caching in HAP-assisted multi-UAV networks using hierarchical federated learning. *J. Phys. Conf. Ser.* **2021**, 1160–1162. [CrossRef]
19. An, S.; Wang, H.; Sun, Y.; Lu, Z.; Yu, Q. Time Domain Multiplexed LoRa Modulation Waveform Design for IoT Communication. *IEEE Commun. Lett.* **2022**, *26*, 838–842.
20. Wei, Z.; Liu, F.; Masouros, C.; Poor, H.V. Fundamentals of Physical Layer Anonymous Communications: Sender Detection and Anonymous Precoding. *IEEE Trans. Wirel. Commun.* **2022**, *21*, 64–79. [CrossRef]
21. Wang, K.; Zhang, R.; Wu, L.; Zhong, Z.; He, L.; Pang, X. Path loss measurement and modeling for low-altitude UAV access channels. In Proceedings of the 2017 IEEE 86th Vehicular Technology Conference (VTC-Fall), Toronto, ON, Canada, 24–27 September 2017; pp. 1–5. [CrossRef]
22. *TR 38.901 V14.0.0*; 3GPP Technical Specification Group Radio Access Networks; Study on Channel Model for Frequencies from 0.5 to 100 GHz (Release14); Technical Report. ETSI: Sophia Antipolis, France, 2017. Available online: https://www.etsi.org/deliver/etsi_tr/138900_138999/138901/14.00.00_60/tr_138901v140000p.pdf (accessed on 5 May 2017).
23. Wang, D.; He, T.; Zhou, F.; Cheng, J.; Zhang, R.; Wu, Q. Outage-Driven Link Selection for Secure Buffer-Aided Networks. *Sci. China Inf. Sci.* **2022**, *65*, 1–16.
24. Huang, Z.; Cheng, X. A General 3D Space-Time-Frequency Non-Stationary Model for 6G Channels. *IEEE Trans. Wirel. Commun.* **2021**, *20*, 535–548. [CrossRef]
25. Zhang, G.; Wu, Q.; Cui, M.; Zhang, R. Securing UAV Communications via Joint Trajectory and Power Control. *IEEE Trans. Wirel. Commun.* **2019**, *18*, 1376–1389. [CrossRef]
26. Kang, Z.; You C.; Zhang, R. 3D Placement for Multi-UAV Relaying: An Iterative Gibbs-Sampling and Block Coordinate Descent Optimization Approach. *IEEE Trans. Commun.* **2021**, *69*, 2047–2062. [CrossRef]

27. Ma, T.; Zhou, H.; Qian, B.; Cheng, N.; Shen, X. UAV-LEO Integrated Backbone: A Ubiquitous Data Collection Approach for B5G Internet of Remote Things Networks. *IEEE J. Sel. Areas Commun.* **2021**, *39*, 3491–3505. [CrossRef]
28. Wu, Y.; Guan, X.; Yang, W.; Wu, Q. UAV Swarm Communication Under Malicious Jamming: Joint Trajectory and Clustering Design. *IEEE Wirel. Commun. Lett.* **2021**, *10*, 2264–2268. [CrossRef]
29. Hu, X.; Zhang, J.; Chung, H.S.; Li, Y.; Liu, O. SamACO: Variable sampling ant colony optimization algorithm for continuous optimization. *IEEE Trans. Syst. Man Cybern. Part B Cybern.* **2010**, *40*, 1555–1566. [CrossRef]